Sensors and Materials, Vol. 36, No. 2 (2024) 523–530
MYU Tokyo

S & M 3540

Scintillation Properties of $Rb_2Cu(Cl,Br)_3$ Crystals

Keishi Yamabayashi,* Kai Okazaki, Daisuke Nakauchi,
Takumi Kato, Noriaki Kawaguchi, and Takayuki Yanagida

Division of Materials Science, Nara Institute of Science and Technology (NAIST),
8916-5 Takayama-Cho, Ikoma City, Nara 630-0192, Japan

(Received October 6, 2023; accepted January 16, 2024)

Keywords: γ-ray detection, phosphor, Hume-Rothery rules, self-trapped excitons, slow cooling method, one-dimensional structure

$Rb_2Cu(Cl,Br)_3$ crystals were synthesized by the slow cooling method and their photoluminescence (PL) and scintillation properties were evaluated. PL emission peaks at 390 nm due to the recombination of excitons were observed, and the PL quantum yields of Rb_2CuCl_3, $Rb_2Cu(Cl_{0.5},Br_{0.5})_3$, and Rb_2CuBr_3 were 91.2, 95.3, and 96.3%, respectively. PL decay curves were approximated using a single exponential function model, and the obtained decay time constants were 15–66 μs. Under X-ray irradiation, the scintillation emission peaks of the samples were observed at 390 nm, and the decay times were 11–63 μs. The afterglow levels at 20 ms after X-ray irradiation were calculated to be 30–450 ppm. Rb_2CuCl_3 showed the highest scintillation light yield of 11000 photons/MeV among the samples when calculated from the pulse height spectra of ^{137}Cs γ-rays (662 keV).

1. Introduction

Scintillators are luminescent materials for ionizing radiation measurements, and they have a function to convert a high-energy quantum to numerous low-energy photons.[1–3] They are generally optically coupled with photomultiplier tubes (PMTs) or photodiodes to convert scintillation photons to electric signals.[3,4] There is a wide range of applications of scintillators, for example, medical imaging,[5] security inspection,[6] natural resource exploration,[7] and materials analysis.[8] The following characteristics are demanded in scintillators for X- and γ-ray detection: high scintillation light yield (*LY*), high density, large effective atomic number, fast scintillation lifetime, and good transparency. However, no scintillators suitable for all the above-mentioned applications have been reported; thus, it is necessary to select scintillators depending on the required performance of the applications. Owing to their excellent optical properties such as high transparency, single-crystal scintillators have been widely studied[9–13] and put into practical applications. For example, $Bi_4Ge_3O_{12}$ (BGO),[14–16] $CdWO_4$ (CWO),[17–19] and Tl:CsI[20–22] have been conventionally used for nondestructive inspections, as represented by X-ray CT and baggage inspections.

*Corresponding author: e-mail: yamabayashi.keishi.yh2@ms.naist.jp
https://doi.org/10.18494/SAM4760

ISSN 0914-4935
https://myukk.org/

Halide single crystals[23–25] as well as oxides[26–29] have been studied for radiation detection, and many scintillators with high *LY* and excellent energy resolution (*DE*) have been discovered. For example, Tl-doped NaI[30–32] and Eu-doped SrI_2[33,34] show excellent luminescence properties; however, these crystals have low chemical stability due to hygroscopicity. In contrast, Cu-based halide compounds are known to have low hygroscopicity.[35,36] In our previous study,[37] we focused on K_2CuBr_3 and Rb_2CuBr_3 and revealed that a continuous solid solution of $(K,Rb)_2CuBr_3$ showed a higher *LY* than Rb_2CuBr_3. Besides, Rb_2CuCl_3 exhibits a high emission intensity under UV and X-ray irradiations;[36–39] however, their scintillation light yields under γ-rays have not been clarified. On the basis of Hume-Rothery rules,[40] the continuous solid solution of $Rb_2Cu(Cl,Br)_3$ can be grown. According to previous studies,[41,42] continuous solid solutions enhanced the scintillation properties owing to changes in bandgap energy or lattice defects. In this study, in addition to Rb_2CuCl_3 and Rb_2CuBr_3, $Rb_2Cu(Cl_{0.5},Br_{0.5})_3$ was developed to enhance the scintillation properties.

2. Materials and Methods

Rb_2CuCl_3, $Rb_2Cu(Cl_{0.5},Br_{0.5})_3$, and Rb_2CuBr_3 were prepared by the slow cooling method. RbCl [$20(1-x)/3$ mmol, 99%, Mitsuwa Chemicals], RbBr ($20x/3$ mmol, 99%, Mitsuwa Chemicals), CuCl [$10(1-x)/3$ mmol, 99.9%, High Purity Chemicals], and CuBr ($10x/3$ mmol, 99.9%, High Purity Chemicals) in the molar ratio of $2-2x:2x:1-x:x$ (x = 0, 0.5, and 1) were dissolved in a mixed solution of HCl aq [$2(1-x)$ mL, 35–37%, Wako Pure Chemical Industries] and HBr aq [$2(1-x)$ mL, 47–49%, Wako Pure Chemical]. Subsequently, the solution was stirred for 2 h at 130 °C, and then H_3PO_2 aq (100 μL, 50%, Fujifilm Wako Pure Chemical) was dropped into the solution to prevent the oxidation of Cu^+. Finally, the solution was slowly cooled from 130 °C to room temperature at a rate of 5 °C/h using a liquid phase synthesizer (Chemi Chemi-300, Shibata) to synthesize single crystals. The grown crystals were washed with 2-propanol (Fujifilm Wako Pure Chemical). The measurement of powder X-ray diffraction (XRD) patterns was performed using a diffractometer (MiniFlex600, Rigaku) to determine crystalline structures. The PL excitation and emission spectra and PL quantum yields (*QY*) were obtained using a Quantaurus-QY (C11347, Hamamatsu Photonics). The PL decay curves were measured using a Quantaurus-τ (C11367, Hamamatsu Photonics). The X-ray-induced scintillation spectra, decay curves, afterglow curves, and pulse height spectra of ^{137}Cs γ-rays (662 keV) were determined using our original setups.[43,44] A shaping amplifier (CP4479, Clear-Pulse) was used for pulse height measurement, and the shaping time was set to 10, 50, and 50 μs for Rb_2CuCl_3, $Rb_2Cu(Cl_{0.5},Br_{0.5})_3$, and Rb_2CuBr_3, respectively.

3. Results and Discussion

Figure 1 shows photographs and XRD patterns of the synthesized samples. Several crystals were precipitated after crystal growth. The obtained samples were colorless and transparent, and the maximum size among the samples was 5–10 mm in length and 1 mm in thickness. The rest of the crystal samples were crushed into powders for XRD measurement. All diffraction peaks

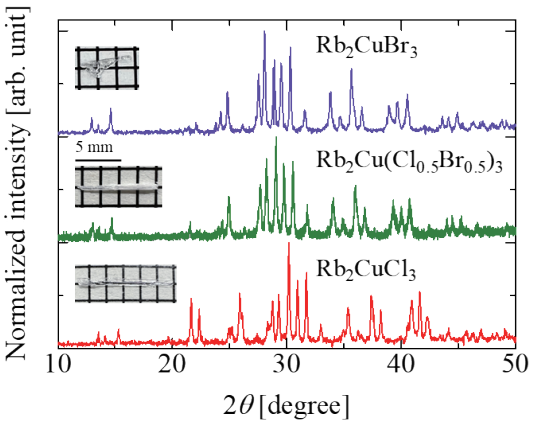

Fig. 1. (Color online) Photographs and XRD patterns of $Rb_2Cu(Cl,Br)_3$ crystals.

of the samples were in good agreement with the reported data of Rb_2CuCl_3[39,45] and the reference data of Rb_2CuBr_3 (JCPDS: 98-015-0295[36]). Therefore, the obtained samples had an orthorhombic crystal system with a space group of *Pnma*.

Figure 2 shows the PL excitation and emission spectra of all the samples. A broad emission peak at 350–550 nm was confirmed under excitation at 250–350 nm. The origin of the emission is the recombination of self-trapped excitons (STEs).[46] When the range of 320–800 nm was monitored under the excitation light of 310 nm, the PL *QY* values of Rb_2CuCl_3, $Rb_2Cu(Cl_{0.5},Br_{0.5})_3$, and Rb_2CuBr_3 were 91.2, 95.3, and 96.3%, respectively. The *QY* of $Rb_2Cu(Cl_{0.5},Br_{0.5})_3$ slightly increased compared with that of Rb_2CuCl_3 via the partial anion substitutions of Cl and Br. In addition, the emission wavelength was shifted to a longer wavelength by Cl replacement.

The insets of Fig. 2 show the PL decay curves of the obtained samples monitored at 390 nm under excitation at 315 nm. The observed decay curves were in good agreement with a single exponential function model. The obtained decay time constants of Rb_2CuCl_3, $Rb_2Cu(Cl_{0.5},Br_{0.5})_3$, and Rb_2CuBr_3 were 15, 31, and 66 μs, respectively, which were comparable to those of previous studies.[36,39,47] The decay time constants decreased as the Cl proportion decreased.

Figures 3 and 4 show the X-ray-induced scintillation spectra and scintillation decay curves, respectively. A broad emission peak at 390 nm was observed, and the peak position shifted toward longer wavelength as the Cl ratio increased. The spectral profile was similar to scintillation in a previous study;[39] therefore, they were considered to be derived from the recombination of STE. All the scintillation decay curves were approximated by a single exponential function model except for the instrumental response function (IRF). The obtained PL and scintillation values were not significantly different and were considered to be within the typical errors.

Figure 5 shows the afterglow curves of the samples after 2 ms irradiation with X-rays. The afterglow level (A) was defined as $A = (I_{20} - I_{BG})/(I_{MAX} - I_{BG})$. I_{20}, I_{MAX}, and I_{BG} are the intensity at 20 ms after X-ray irradiation for 2 ms, the intensity during X-ray irradiation, and the

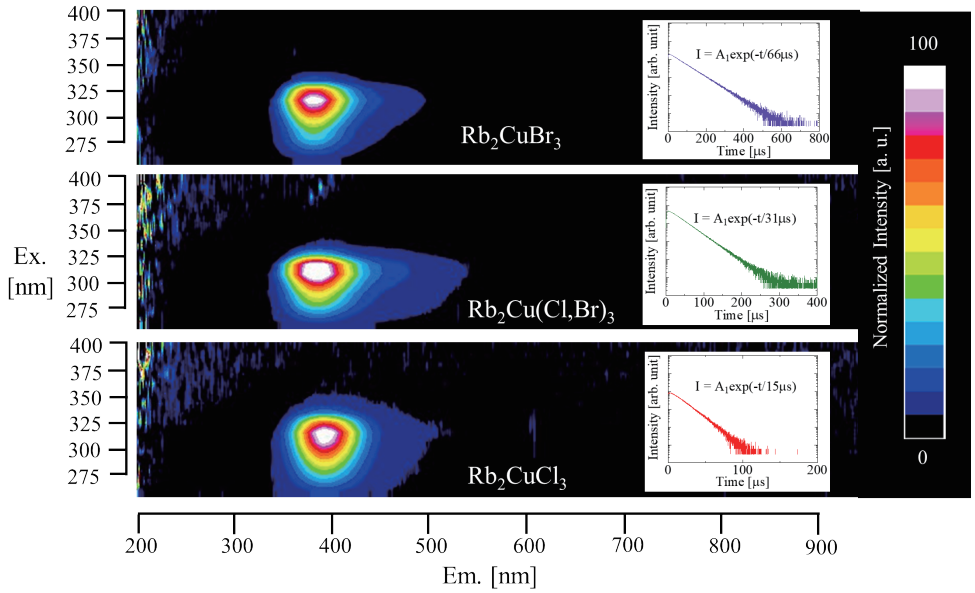

Fig. 2. (Color online) PL excitation and emission spectra of $Rb_2Cu(Cl,Br)_3$. Horizontal and vertical axes indicate emission and excitation wavelengths, respectively. Insets show PL decay curves measured under excitation at 315 nm and monitored at 390 nm.

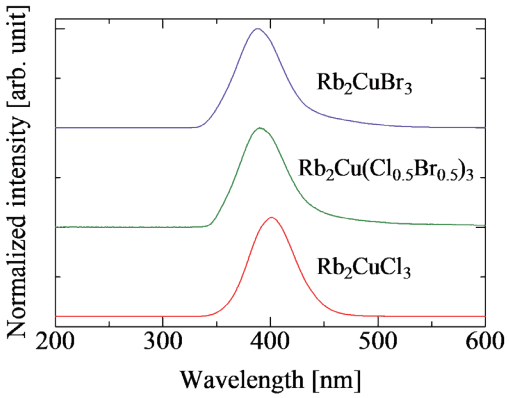

Fig. 3. (Color online) X-ray-induced scintillation spectra of $Rb_2Cu(Cl,Br)_3$ crystals.

background intensity before X-ray irradiation, respectively. The obtained A values of Rb_2CuCl_3, $Rb_2Cu(Cl_{0.5},Br_{0.5})_3$, and Rb_2CuBr_3 were 30, 36, and 450 ppm, respectively. These values significantly decreased as the Cl ratio increased. In addition, the values of Rb_2CuCl_3 and $Rb_2Cu(Cl_{0.5},Br_{0.5})_3$ were lower than that of Tl:CsI (300 ppm), which has been one of the conventional halide scintillators,[48] and comparable to that of $Bi_4Ge_3O_{12}$ (10 ppm),[48] a scintillator for X-ray detection under the same measurement condition.

Figure 6 shows the pulse height spectra of ^{137}Cs γ-rays measured using the samples and CWO as a reference sample, which shows LY of 15800 photons/MeV.[49] All the samples exhibited a photoabsorption peak. The peak channel was determined by Gaussian approximation, and the

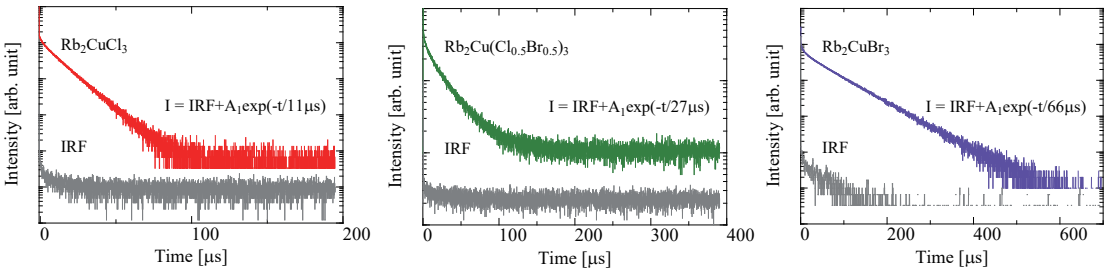

Fig. 4. (Color online) X-ray-induced scintillation decay curves of $Rb_2Cu(Cl,Br)_3$ crystals.

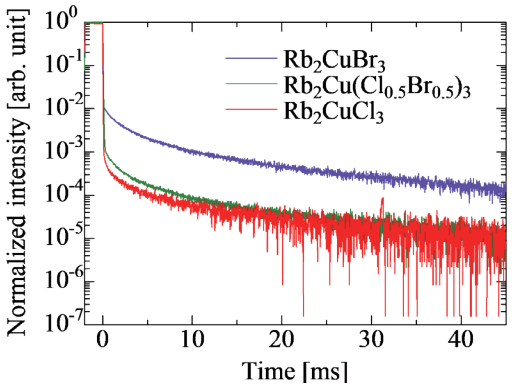

Fig. 5. (Color online) Afterglow curves of $Rb_2Cu(Cl,Br)_3$ crystals.

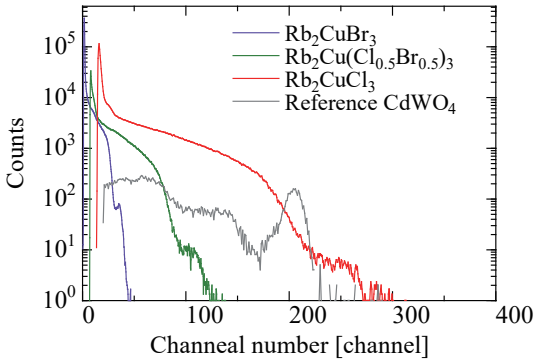

Fig. 6. (Color online) Pulse height spectra of ^{137}Cs γ-ray (662 keV) measured using $Rb_2Cu(Cl,Br)_3$ crystals and CWO as a reference.

calculated *LY* values of Rb_2CuCl_3, $Rb_2Cu(Cl_{0.5},Br_{0.5})_3$, and Rb_2CuBr_3 were 11000, 4900, and 1500 photons/MeV, respectively, after corrections of the PMT sensitivity. In addition, the *DE* values at 662 keV for Rb_2CuCl_3, $Rb_2Cu(Cl_{0.5},Br_{0.5})_3$, and Rb_2CuBr_3 were 10.4, 10.8, and 12.1%, respectively. The difference in the estimation of *LY* was attributed to the different measurement methods used. In a previous study,[39] the *LY* of Rb_2CuCl_3 was estimated from the scintillation spectrum, whereas the current work used the pulse height spectrum. Rb_2CuCl_3 showed the highest *LY* and the lowest *A* among the samples. They did not follow the tendency of *QY*. In general, scintillation and storage-type luminescence properties such as afterglow show an inverse relationship.[50,51] The *A* values of Cl-containing samples were lower than those of $Rb_2Cu(Cl_{0.5},Br_{0.5})_3$ and Rb_2CuBr_3, and the trend was consistent with the relationship.

4. Conclusions

Continuous solid solutions of $Rb_2Cu(Cl_{0.5},Br_{0.5})_3$ crystals were successfully synthesized by the slow cooling method. In the PL and scintillation spectra, a broad emission peak was observed at 390 nm, and the emission mechanism was attributed to the recombination of STEs. The PL

and scintillation decay curves were approximated using a single exponential function model, and the obtained decay constants (11–66 μs) decreased as the Cl proportion increased. *A* was improved from 450 ppm (Rb_2CuBr_3) to 36 ppm [$Rb_2Cu(Cl,Br)_3$] and 30 ppm (Rb_2CuCl_3) by changing the anion part to Cl from Br. The *LY* values of the samples tended to increase as the Cl ratio in the composition increased; the maximum *LY* was 11000 photons/MeV calculated for Rb_2CuCl_3. As a comprehensive result, the unsubstituted sample Rb_2CuCl_3 showed the best scintillation properties among the samples. The *A* and *LY* of Rb_2CuCl_3 were comparable to those of BGO, which is one of the representative commercially available scintillators for security and anticompton spectrometers.[52] Therefore, Rb_2CuCl_3 can be a promising material for the above applications.

Acknowledgments

This work was supported by Grants-in-Aid for Scientific Research A (22H00309), Scientific Research B (21H03733, 21H03736, and 22H03872), and Exploratory Research (22K18997) from the Japan Society for the Promotion of Science. JST A-STEP, Foundation from Cooperative Research Project of the Research Center for Biomedical Engineering, Kazuchika Okura Memorial Foundation, Asahi Glass Foundation, Nakatani Foundation, and Konica Minolta Science and Technology Foundation are also acknowledged.

References

1 C. W. E. Van Eijk: Nucl. Instrum. Methods Phys. Res., Sect. A **460** (2001) 1. https://doi.org/10.1016/S0168-9002(00)01088-3
2 A. Lempicki, A. J. Wojtowicz, and E. Berman: Nucl. Instrum. Methods Phys. Res., Sect. A **333** (1993) 304. https://doi.org/10.1016/0168-9002(93)91170-R
3 T. Yanagida, T. Kato, D. Nakauchi, and N. Kawaguchi: J. Appl. Phys. **62** (2022) 010508. https://doi.org/10.35848/1347-4065/ac9026
4 M. Koshimizu: Jpn. J. Appl. Phys. **62** (2022) 010503. https://doi.org/10.35848/1347-4065/ac94fe
5 P. Lecoq: Nucl. Instrum. Methods Phys. Res., Sect. A **809** (2016) 130. https://doi.org/10.1016/j.nima.2015.08.041
6 J. Glodo, Y. Wang, R. Shawgo, C. Brecher, R. H. Hawrami, J. Tower, and K. S. Shah: Phys. Procedia **90** (2017) 285. https://doi.org/10.1016/j.phpro.2017.09.012
7 C. L. Melcher: Nucl. Instrum. Methods Phys. Res., Sect. B **40**–**41** (1989) 1214. https://doi.org/10.1016/0168-583X(89)90622-8
8 V. V. Nagarkar, T. K. Gupta, S. R. Miller, Y. Klugerman, M. R. Squillante, and G. Entine: IEEE Trans. Nucl. Sci. **45** (1998) 492. https://doi.org/10.1109/23.682433
9 P. Kantuptim, D. Nakauchi, T. Kato, N. Kawaguchi, and T. Yanagida: Sens. Mater. **34** (2022) 603. https://doi.org/10.18494/SAM3690
10 K. Okazaki, D. Onoda, D. Nakauchi, N. Kawano, H. Fukushima, T. Kato, N. Kawaguchi, and T. Yanagida: Sens. Mater. **34** (2022) 575. https://doi.org/10.18494/SAM3678
11 Y. Fujimoto and K. Asai: Jpn. J. Appl. Phys. **62** (2022) 010605. https://doi.org/10.35848/1347-4065/ac9348
12 D. Nakauchi, T. Kato, N. Kawaguchi, and T. Yanagida: Jpn. J. Appl. Phys. **62** (2022) 010607. https://doi.org/10.35848/1347-4065/ac9181
13 H. Fukushima, D. Nakauchi, T. Kato, N. Kawaguchi, and T. Yanagida: Jpn. J. Appl. Phys. **62** (2022) 010506. https://doi.org/10.35848/1347-4065/ac9105
14 K. Okazaki, D. Nakauchi, H. Fukushima, T. Kato, N. Kawaguchi, and T. Yanagida: Sens. Mater. **35** (2023) 459. https://doi.org/10.18494/SAM4144
15 J. Gironnet, V. B. Mikhailik, H. Kraus, P. de Marcillac, and N. Coron: Nucl. Instrum. Methods Phys. Res., Sect. A **594** (2008) 358. https://doi.org/10.1016/j.nima.2008.07.008

16 K. Takagi, T. Oi, T. Fukazawa, M. Ishii, and S. Akiyama: J. Cryst. Growth **52** (1981) 584. https://doi.org/10.1016/0022-0248(81)90345-6
17 S. P. Burachas, F. A. Danevich, A. S. Georgadze, H. V. Klapdor-Kleingrothaus, V. V. Kobychev, B. N. Kropivyansky, V. N. Kuts, A. Muller, V. V. Muzalevsky, A. S. Nikolaiko, O. A. Ponkratenko, V. D. Ryzhikov, A. S. Sai, I. M. Solsky, V. I. Tretyak, and Y. G. Zdesenko: Nucl. Instrum. Methods Phys. Res., Sect. A **369** (1996) 164. https://doi.org/10.1016/0168-9002(95)00675-3
18 A. Phunpueok, V. Thongpool, and S. Jaiyen: J. Phys. Conf. Ser. **1380** (2019) 012128. https://doi.org/10.1088/1742-6596/1380/1/012128
19 D. V. Poda, A. S. Barabash, P. Belli, R. Bernabei, R. S. Boiko, V. B. Brudanin, F. Cappella, V. Caracciolo, S. Castellano, R. Cerulli, D. M. Chernyak, F. A. Danevich, S. D'Angelo, V. Y. Degoda, M. L. Di Vacri, A. E. Dossovitskiy, E. N. Galashov, A. Incicchitti, V. V. Kobychev, S. I. Konovalov, G. P. Kovtun, M. Laubenstein, A. L. Mikhlin, V. M. Mokina, A. S. Nikolaiko, S. Nisi, R. B. Podviyanuk, O. G. Polischuk, A. P. Shcherban, V. N. Shlegel, D. A. Solopikhin, V. I. Tretyak, V. I. Umatov, Y. V. Vasiliev, and V. D. Virich: Radiat. Meas. **56** (2013) 66. https://doi.org/10.1016/j.radmeas.2013.02.017
20 M. R. Farukhi: IEEE Trans. Nucl. Sci. **29** (1982) 1237. https://doi.org/10.1109/TNS.1982.4336345
21 W. Mengesha: IEEE Trans. Nucl. Sci. **45** (1998) 456. https://doi.org/10.1109/23.682426
22 D. W. Aitken, B. L. Beron, G. Yenicay, and H. R. Zulliger: IEEE Trans. Nucl. Sci. **14** (1967) 468. https://doi.org/10.1109/TNS.1967.4324457
23 Y. Fujimoto, D. Nakauchi, T. Yanagida, M. Koshimizu, and K. Asai: Sens. Mater. **34** (2022) 629. https://doi.org/10.18494/SAM3693
24 D. Nakauchi, Y. Fujimoto, T. Kato, N. Kawaguchi, and T. Yanagida: Crystals **12** (2022) 517. https://doi.org/10.3390/cryst12040517
25 D. Onoda, M. Akatsuka, N. Kawano, T. Kato, D. Nakauchi, N. Kawaguchi, and T. Yanagida: Sens. Mater. **34** (2022) 585. https://doi.org/10.18494/SAM3679
26 H. Fukushima, D. Nakauchi, T. Kato, N. Kawaguchi, and T. Yanagida: Sens. Mater. **35** (2023) 429. https://doi.org/10.18494/SAM4139
27 P. Kantuptim, T. Kato, D. Nakauchi, N. Kawaguchi, K. Watanabe, and T. Yanagida: Sens. Mater. **35** (2023) 451. https://doi.org/10.18494/SAM4141
28 T. Yanagida, T. Kato, D. Nakauchi, and N. Kawaguchi: Sens. Mater. **34** (2022) 595. https://doi.org/10.18494/SAM3684
29 D. Nakauchi, H. Fukushima, T. Kato, N. Kawaguchi, and T. Yanagida: Sens. Mater. **34** (2022) 611. https://doi.org/10.18494/SAM3696
30 R. Hawrami, E. Ariesanti, A. Farsoni, D. Szydel, and H. Sabet: Crystals **12** (2022) 1517. https://doi.org/10.3390/cryst12111517
31 M. Gascón, S. Lam, S. Wang, S. Curtarolo, and R. S. Feigelson: Radiat. Meas. **56** (2013) 70. https://doi.org/10.1016/j.radmeas.2013.04.017
32 J. Brechtl, X. Xie, R. Feng, G. Wang, C. Melcher, M. Zhuravleva, and P. K. Liaw: J. Mater. Sci. Technol. **153** (2023) 120. https://doi.org/10.1016/j.jmst.2022.12.047
33 A. Smerechuk, E. Galenin, V. Nesterkina, O. Sidletskiy, and C. Dujardin: J. Cryst. Growth **521** (2019) 41. https://doi.org/10.1016/j.jcrysgro.2019.05.031
34 E. V. Van Loef, C. M. Wilson, N. J. Cherepy, G. Hull, S. A. Payne, W. S. Choong, W. W. Moses, and K. S. Shah: IEEE Trans. Nucl. Sci. **56** (2009) 869. https://doi.org/10.1109/TNS.2009.2013947
35 T. D. Creason, T. M. McWhorter, Z. Bell, M. H. Du, and B. Saparov: Chem. Mater. **32** (2020) 6197. https://doi.org/10.1021/acs.chemmater.0c02098
36 B. Yang, L. Yin, G. Niu, J. H. Yuan, K. H. Xue, Z. Tan, X. S. Miao, M. Niu, X. Du, H. Song, E. Lifshitz, and J. Tang: Adv. Mater. **31** (2019) 1904711. https://doi.org/10.1002/adma.201904711
37 K. Yamabayashi, K. Okazaki, D. Nakauchi, T. Kato, N. Kawaguchi, and T. Yanagida: Radiat. Phys. Chem. **214** (2024) 111292. https://doi.org/10.1016/j.radphyschem.2023.111292
38 W. Naewthong, W. Juntapo, R. Amarit, K. Duangkanya, S. Sumriddetchkajorn, T. Rungseesumran, N. Kamwang, Y. Tariwong, J. Kaewkhao, A. Kopwitthaya, and A. Kopwitthaya: Opt. Mater. Express **12** (2022) 308. https://doi.org/10.1364/OME.444631
39 X. Zhao, G. Niu, J. Zhu, B. Yang, J. H. Yuan, S. Li, W. Gao, Q. Hu, L. Yin, K. H. Xue, E. Lifshitz, X. Miao, and J. Tang: J. Phys. Chem. **11** (2020) 1873. https://doi.org/10.1021/acs.jpclett.0c00161
40 W. Hume-Rothery, P. W. Reynolds, and G. V. Raynor: Nature **146** (1940) 528. https://doi.org/10.1038/146528a0
41 M. Arai, Y. Fujimoto, M. Koshimizu, H. Kimura, T. Yanagida, and K. Asai: Mater. Res. Bull. **120** (2019) 110589. https://doi.org/10.1016/j.materresbull.2019.110589

42 T. Hayashi, K. Ichiba, D. Nakauchi, K. Watanabe, T. Kato, N. Kawaguchi, and T. Yanagida: J. Lumin. **255** (2023) 119614. https://doi.org/10.1016/j.jlumin.2022.119614
43 T. Yanagida, K. Kamada, Y. Fujimoto, H. Yagi, and T. Yanagitani: Opt. Mater. **35** (2013) 2480. https://doi.org/10.1016/j.optmat.2013.07.002
44 T. Yanagida, Y. Fujimoto, T. Ito, K. Uchiyama, and K. Mori: Appl. Phys. Express **7** (2014) 062401. https://doi.org/10.7567/APEX.7.062401
45 K. X. Xu, Z. Zhou, and J. Zhang: J. Phys. Chem. Lett. **14** (2023) 32. https://doi.org/https://doi.org/10.1021/acs.jpclett.2c03514
46 T. D. Creason, A. Yangui, R. Roccanova, A. Strom, M. H. Du, and B. Saparov: Adv. Opt. Mater. **8** (2020) 1901338. https://doi.org/10.1002/adom.201901338
47 S. Zhao, Z. Jia, Y. Huang, Q. Qian, Q. Lin, Z. Zang, S. Zhao, Y. Huang, Q. Qian, Z. Zang, Z. Jia, and Q. Lin: Adv. Funct. Mater. (2023) 2305858. https://doi.org/10.1002/adfm.202305858
48 D. Nakauchi, T. Kato, N. Kawaguchi, and T. Yanagida: Appl. Phys. Express **13** (2020) 122001. https://doi.org/10.35848/1882-0786/abc574
49 W. Klamra, T. Szczesniak, M. Moszynski, J. Iwanowska, L. Swiderski, A. Syntfeld-Kazuch, V. N. Shlegel, Y. V. Vasiliev, and E. N. Galashov: J. Instrum. **7** (2012) P03011. https://doi.org/10.1088/1748-0221/7/03/P03011
50 T. Yanagida: J. Lumin. **169** (2016) 544. https://doi.org/10.1016/j.jlumin.2015.01.006
51 T. Yanagida: Proc. Jpn. Acad. Ser. B **94** (2018) 75. https://doi.org/10.2183/pjab.94.007
52 I. Holl, E. Lorenz, and G. Mageras: IEEE Trans. Nucl. Sci. **35** (1988) 105. https://doi.org/10.1109/23.12684